

“Rainbow” Storage Ring Nuclear Transmutation with Spin Control Capability

Richard Talman

Laboratory for Elementary-Particle Physics
Cornell University, Ithaca, NY, USA

Weak-focusing Storage Ring Nuclear
Transmutation Slides, July 15, 2023

2 Outline for Storage Ring Nuclear Transmutation Lecture

Storage ring nuclear transmutation as nuclear power source

“Rainbow” nuclear scattering threshold pattern

Superimposed electric and magnetic storage ring bending

Rear end collisions

Deuteron stripping processes

Quantum mechanical determination of nuclear scattering patterns

Preparatory to the measurement of spin-dependence

“Rainbow” kinematic plots

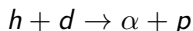
Estimated rate of power generation

“Pure physics” study of isotope conversion events

Pure physics goals

3 Storage ring nuclear transmutation as nuclear power source

- ▶ A preliminary goal is to demonstrate electrical power generation using deuteron (d) and He3 nuclei (helion, h) beams for the nuclear transmutation process



producing α -particles and protons.

- ▶ Low-Z nuclear isotope pairs, say h and d , having more or less the same charge to momentum ratios, but different velocities, can co-circulate in the same “circular” storage ring provided the bending is provided by superimposed magnetic and electric bending.
- ▶ This takes advantage of the different velocity dependence of magnetic and electric bending forces.
- ▶ With a helion to deuteron velocity ratio $v_h/v_d = 8/7$, a helion bunch on every eighth turn will “lap” (and pass through) a deuteron bunch that is just completing its seventh full turn.

4 Valuable comment due to Christian Carli, (3 July, 2023)

- ▶ With $7 \times 8 = 56$, by choosing the RF frequency to be the 56'th harmonic of a standard base frequency, f_{base} , itself a harmonic number h_n multiple $f_{\text{base}} = h_n f_{\text{rev}}$. of the revolution frequency, both circulating beams can be bunched by a single RF cavity, in spite of their different velocities.
- ▶ This does, however, restrict the possible collision point beam intersection point (IP) locations relative to the RF cavity.

- ▶ With judicious adjustment this will always occur at the ring location of a full acceptance interaction detector/polarimeter.
- ▶ In this configuration the rest mass of the h, d system will be fine-tunable on a KeV scale, for example barely exceeding the threshold of the $h + d \rightarrow \alpha + p$ channel.
- ▶ To the extent that spin dependence is insignificant, this radiation pattern can be described as a “rainbow” circular ring (or rather cone) especially of the more massive (α -particles) emerging from, and centered on, the common beam axis.
- ▶ This “view” has not been observed previously in nuclear scattering since it requires a “rear end” collision in which a more massive but faster moving (in the laboratory) helion overtakes a lower mass but slower moving deuteron.
- ▶ In principle, the final state beams can be separated and their energies recovered with high efficiency without violating Liouville's principle.

- ▶ Of all the nuclear candidates for fusion power this $h + d$ channel is (marginally) the most exothermic as well as being “aneutronic”.
- ▶ Conventional thermonuclear power generation is restricted to the deuteron/triton channel $d + t \rightarrow n + \alpha$ process, because of its relatively low nuclear ignition temperature.
- ▶ Though almost equivalently exothermic, this channel produces neutrons in the final state.
- ▶ These neutrons will inevitably cause unacceptably great radiation damage to the delicate apparatus needed to produce the requisite high ignition temperature.
- ▶ Proposed here is storage ring capable of producing and detecting $d + h \rightarrow \alpha + p$ nuclear transmutation events, with emphasis on polarization dependence.

7 Exothermic nuclear transmutation channels

Candidate reactions		
Reaction	Ignition T [keV]	Cross-section $\langle\sigma v\rangle/T^2$ [$\text{m}^3/\text{s}/\text{keV}^2$]
${}^2_1\text{D}-{}^3_1\text{T}$	13.6	1.24×10^{-24}
${}^2_1\text{D}-{}^3_2\text{He}$	58	2.24×10^{-26}

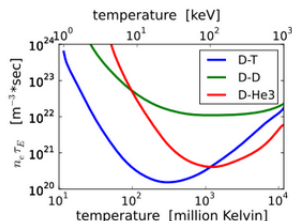


Figure 1: From 2021 Wikipedia article, “Aneutronic fusion”: **Left:** Comparison of potential thermonuclear fuels; **Right:** “Lawson triple product” empirical expression for thermonuclear effectiveness as a function of temperature, in Kelvin units (bottom scale) and KeV (top scale). All three of these channels can be studied in detail.

$${}^2_1\text{D} - {}^3_1\text{T} : \quad t + d \rightarrow \alpha + n, \quad (+17.6 \text{ MeV}) \quad (1)$$

$${}^2_1\text{D} - {}^3_2\text{He} : \quad h + d \rightarrow \alpha + p \quad (+18.3 \text{ MeV}) \quad (2)$$

$${}^2_1\text{D} - {}^2_1\text{D} : \quad d + d \rightarrow h + n \quad (+3.2 \text{ MeV}) \quad (3)$$

9 PTR prototype storage ring

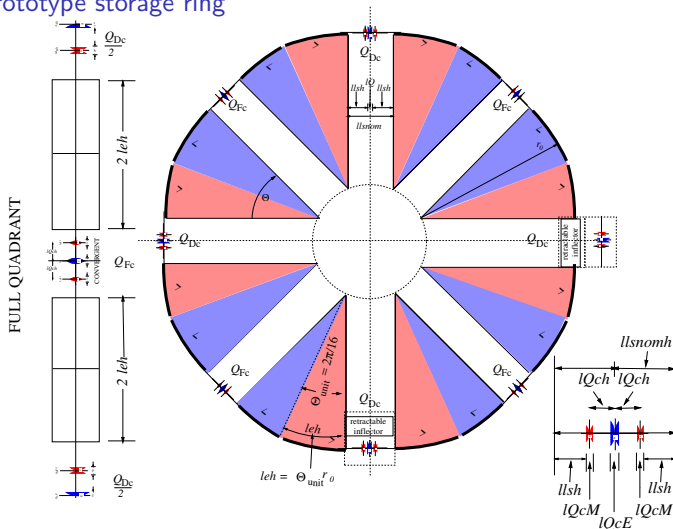


Figure 3: Lattice layouts for PTR, the proposed prototype nuclear transmutation storage ring prototype; “compromise” quadrupole lower right. The circumference is 102 m.

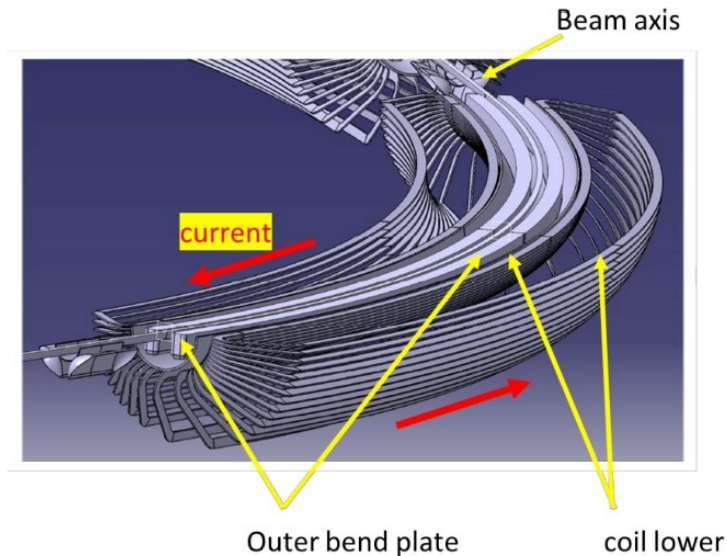


Figure 4: Perspective mock-up of one sector of PTR, the superimposed E/M prototype ring. Two “short-circuited ends” $\cos \theta$ -dipoles surround the beam tube, within which the capacitor plates are accommodated.

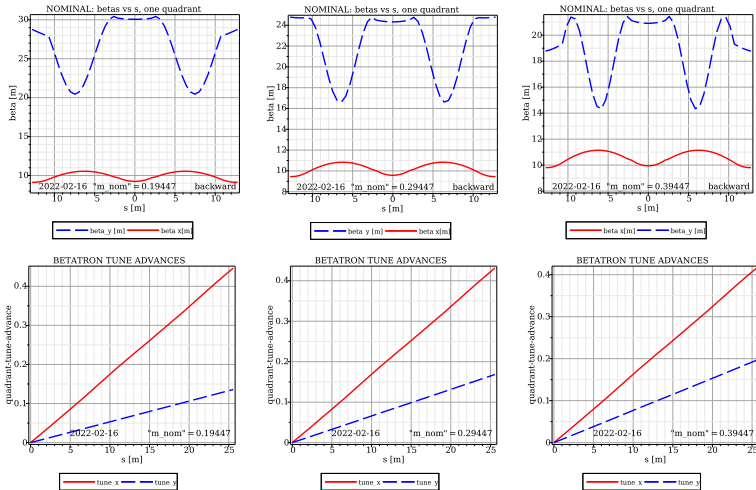
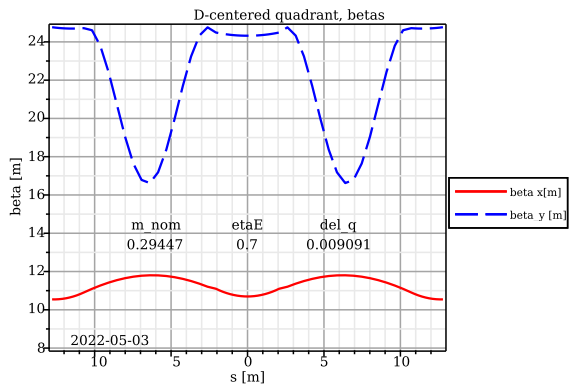
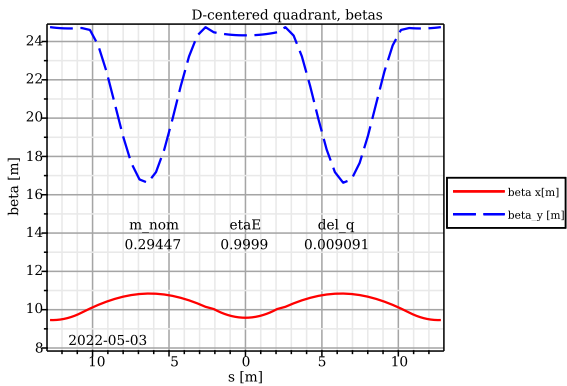


Figure 5: PTR optical functions for one quadrant centered at a D-focusing quadrupole straight section, with all quadrupole strengths set to zero. **Left:** over-focused, **Right:** under-focused, **Center:** **correctly-focused** betatron tune advances plotted against longitudinal coordinate s . Full ring tunes are four times the right hand intercepts.





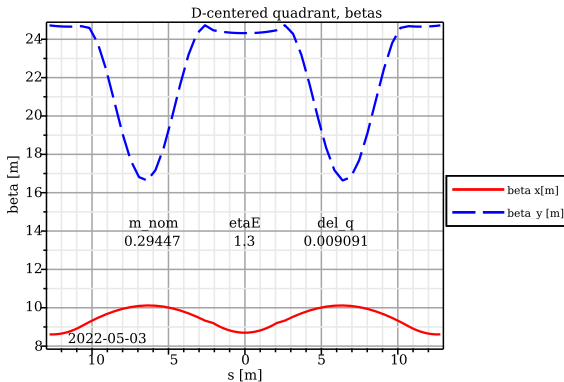


Figure 6: PTR beta functions with $m_{nom} = 0.29447$, corresponding to the “tuned-up” value for the central case in Fig. 5 **“Rainbow” nuclear scattering threshold pattern** Doc-Start. In this configuration, in spite of being “thick lenses” the intervening bends act like drift sections (of length not equal to the arc length in general). Optically the full ring then acts like a separated function FODO lattice with alternating gradient lumped quadrupole with focusing strength $del_q = 0.1/r_0 = 0.009091/\text{m}$. Fractional electric field bending fraction η_E varies from 0.7 in the top graph to 1.3 in the bottom. This variation leaves β_y unchanged, but

causes β_x to vary (approximately proportional to $1/\sqrt{\eta E}$).

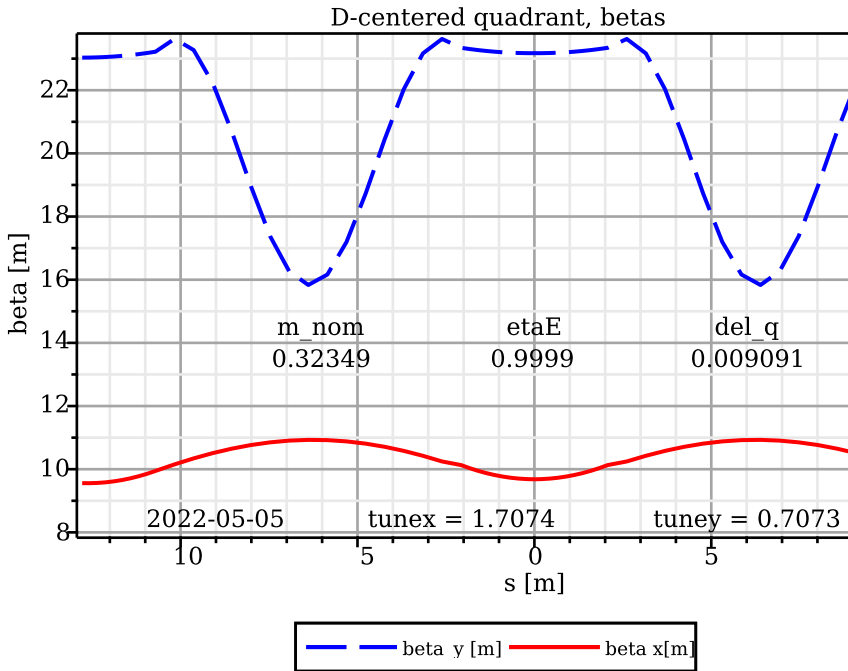


Figure 7: For essentially all electric bending ($\eta_E = 0.9999$), and quite weak lumped quadrupole tuning ($del_q = 0.009091 \text{ m}^{-1}$), the horizontal and vertical fractional tunes have been made equal (1.7073). In this condition, by itself, the presence of betatron motion causes no beam depolarization.

11 “Rainbow” nuclear scattering pattern

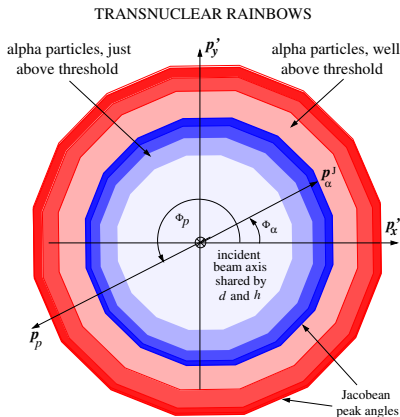


Figure 8: Transnuclear “rainbows” produced in the reaction $h + d \rightarrow \alpha + p$. Shading represents scattered differential cross section. Rainbow radii increase proportional to incident energy excess above threshold. Superscript “J” labels the rainbow divergence edge caused by the vanishing Jacobean at the maximum laboratory scattering angle.

12 Superimposed electric and magnetic storage ring bending

- ▶ As first suggested by Koop, in the context of EDM measurement,
- ▶ it is possible, with superimposed electric and magnetic bending, for beams of two different particle types to circulate simultaneously
- ▶ This opens the possibility of “rear-end” collisions occurring while a fast bunch is passing through a slow bunch.
- ▶ Bunches of the same beam type can also circulate simultaneously if they have different momenta.

Storage ring nuclear transmutation at BNL

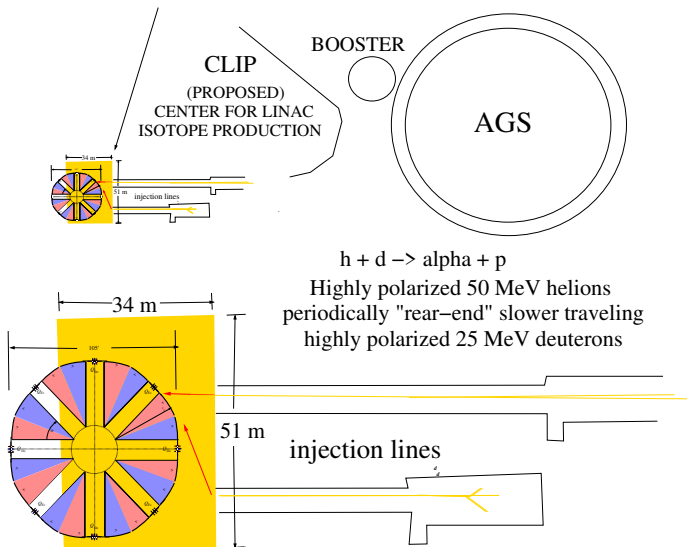


Figure 9: Above: Tentative CLIP location near AGS at BNL; **Below:** Blown-up image of transmutation ring within CLIP.

14 Carbon foil, full aperture stopping-proton tracker/polarimeter

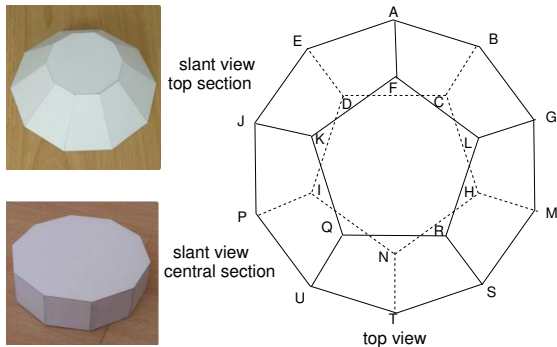
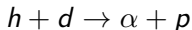


Figure 10: Artist's conception top view of an almost full-acceptance tracking/stopping/polarimeter at the storage ring intersection point IP. Their dodecahedral faces subtend roughly equal solid angles. The figures shown on the left are slant views of horizontal slices. To accommodate passage of the colliding beams there is reduced aperture in the forward (and backward, if two-way circulation is allowed) directions.

15 Rear end $h + d \rightarrow \alpha + p$ collisions

- ▶ With primary beam consisting of fast helions and secondary beam slower deuterons, the helion bunches will “lap” and pass through the slower deuteron bunches, causing h,d “rear end” collisions periodically.
- ▶ In this configuration the center of mass (CM) is in a modestly relativistic moving frame, in which the particle CM kinetic energies are in the range roughly, from 100 KeV to 1 MeV, while their laboratory energies are in the range roughly, from 10 MeV to hundreds of MeV.
- ▶ The center of mass will be traveling, typically, at a velocity such as $\beta = 0.16$, that of a 25 MeV kinetic energy deuteron in the laboratory.
- ▶ The center of mass kinetic energies (where their momenta are equal and opposite) are (roughly) 300 KeV, which is close to the Coulomb barrier height for the nuclear scattering channel,



16 Centering the collision point location

bm 1	beta1	Qs1	KE1 MeV	E0 MV/m	betaB0 mT	beta2	Qs2	KE2 MeV	beta*	gamma*	M* GeV	Q12 KeV	7*bratio	bm 2
h	0.1769	-0.665	45.000	4.64395	-3.30871	0.1547	-1.096	22.864	0.16804	1.01443	4.68430	292.18399	8.00287	d
h	0.1788	-0.666	46.000	4.74965	-3.36417	0.1564	-1.097	23.373	0.16986	1.01475	4.68430	298.53366	8.00219	d
h	0.1807	-0.666	47.000	4.85547	-3.41966	0.1581	-1.097	23.882	0.17166	1.01507	4.68431	304.87722	8.00151	d
h	0.1826	-0.666	48.000	4.96139	-3.47518	0.1597	-1.097	24.391	0.17343	1.01539	4.68432	311.21468	8.00083	d
h	0.1844	-0.666	49.000	5.06742	-3.53074	0.1613	-1.098	24.901	0.17519	1.01571	4.68432	317.54605	8.00015	d
h	0.1862	-0.666	50.000	5.17355	-3.58633	0.1630	-1.098	25.410	0.17693	1.01603	4.68433	323.87133	7.99947	d
h	0.1880	-0.667	51.000	5.27980	-3.64198	0.1645	-1.099	25.920	0.17865	1.01635	4.68433	330.19053	7.99879	d
h	0.1898	-0.667	52.000	5.38616	-3.69767	0.1661	-1.099	26.429	0.18035	1.01667	4.68434	336.50366	7.99811	d
h	0.1916	-0.667	53.000	5.49263	-3.75342	0.1677	-1.099	26.939	0.18204	1.01699	4.68435	342.81073	7.99744	d

Table 1: Fine-grain scan to center the collision point for KE1=49 MeV helion energy and 25 MeV deuteron energy. The electric/magnetic field ratio then produces perfect $\beta_h/\beta_d=8/7$ velocity ratio so that, for every 7 deuteron turns, the helion makes 8 turns. Notice, also, the approximate match of Q12=317 KeV in this table, with $V_{d,He3}=313.1$ KeV. This matches the incident kinetic energy to the value required to surmount the repulsive Coulomb barrier.

- ▶ The columns labeled Q_s are spin tunes. In this talk nothing will be said about polarization, but polarized beams are anticipated.
- ▶ A major thrust of the proposal is the capability of experimental measurement of spin dependence in nuclear transmutation.

17 $h + d \rightarrow \alpha + p$ kinematics

bm 1	m1 GeV	G1	q1	beta1	Qs1	KE1 MeV	E0 MV/m	betaB0 mT	m2 GeV	G2	q2	beta2	KE2 MeV	bratio	bm
h	2.8084	-4.1842	2	0.18440	-6.662e-01	49.0000	5.0674	-3.5307	1.8756	-0.1430	1	-0.18144	31.6569	-0.98396	d
h	2.8084	-4.1842	2	0.18440	-6.662e-01	49.0000	5.0674	-3.5307	1.8756	-0.1430	1	0.16135	24.9007	0.87498	d

Table 2: Parameters for co- and contra-traveling helion and deuteron beams, for identical settings of magnetic and electric bending, appropriate, respectively, for head-on and rear-end collisions.

bm 3	m3 GeV	G3	q3	Q34_min MeV	KE3_eff MeV	KE4_eff MeV	E0 MV/m	betaB0 mT	m4 GeV	G4	q4	bm
α	3.7274	0.0000	2	18.67	3.78	14.89	5.0674	-3.5307	0.9383	1.7928	1	p

Table 3: Matching parameters for α -particle and proton final state channel.

18 Deuteron stripping processes

- ▶ The $h + d \rightarrow \alpha + p$ process is a “stripping” or “direct nuclear” reaction, well described by semi-classical kinematic reasoning.
- ▶ This approach is especially applicable to deuterons because of their large radius and weakly coupled proton and neutron pioneered by Butler in 1951
- ▶ The stripping analysis bears directly on the recovery efficiency of energy transferred from helion to α -particle associated with the huge, 28 MeV, α -particle binding energy.
- ▶ To be commercially viable the exothermic energy released in the nuclear transmutation needs to be recovered with high efficiency.

- ▶ Most of this energy simply adds to the heavy, newly produced α -particle energy
- ▶ For economically effective electrical power generation it is essential to recover most of the 92 MeV of outgoing kinetic energy, rather than just the 18.3 MeV, of exothermically released energy.
- ▶ Most of this energy will be recoverable as electrical power using energy recovery linac (ERL) technology,
- ▶ It is theoretically possible to recover most of this energy in the form of electrical energy for every captured α -particle.
- ▶ But the fraction of the final state energy carried by final state protons can only be collected as thermal energy.

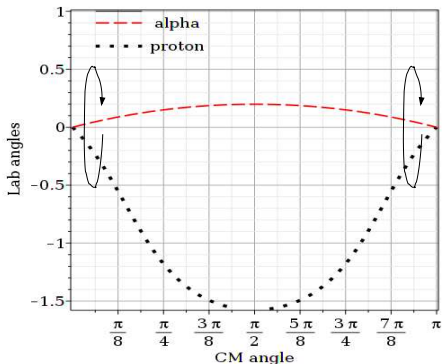
20 Quantum mechanical determination of nuclear scattering patterns

- ▶ Any calculation of the probabilities of conversion from one set of nuclear particle species into another is necessarily quantum mechanical (QM).
- ▶ But for initial state collinearity and two-body final states the calculation is highly constrained by symmetry and conservation law requirements.
- ▶ For the basic process described in this paper sophisticated QM machinery is superfluous.
- ▶ The present paper amounts to a first cut preparation before performing subsequent spin-dependent measurements.

21 Preparation for measurement of spin-dependence

- ▶ The proposed facility will have the capability of establishing pure incident state spin states and measuring all final state polarizations.
- ▶ These can be investigated theoretically only by using the full QM machinery to calculate the relevant transfer matrices.
- ▶ None of this is covered in this presentation which, basically, accepts transfer matrices as being identity matrices.
- ▶ This reduces the Fermi scattering formalism to a density of states calculation, with no need for more refined QM machinery.
- ▶ Near threshold the angular distributions are isotropic.
- ▶ With two-body final state limitation, along with collinear incident beams, both final state particle orbits lie in a plane containing the beam axis and oriented by a single azimuthal angle.
- ▶ By cylindrical symmetry it would be theoretically unnecessary even to label this azimuthal angle; in fact, in Figure 3, one such plane can be labeled by either Φ_α or Φ_p .

22 “Rainbow” kinematic plot



- ▶ This planar plot of laboratory angle vs CM angle should be visualized as if rolled around its horizontal axis, as indicated by the rotation arrows.
- ▶ α particles are contained within a cone half-angle of 0.2 radians.
- ▶ At the α -particle maximum scattering angle the vanishing slope in this view produces a “Jacobean peak” at the rim of the rainbow shown previously.
- ▶ The rainbow radius increases with incident energy, say from blue to red in earlier rainbow plot.

23 “Rainbow” nuclear scattering pattern (repeated)

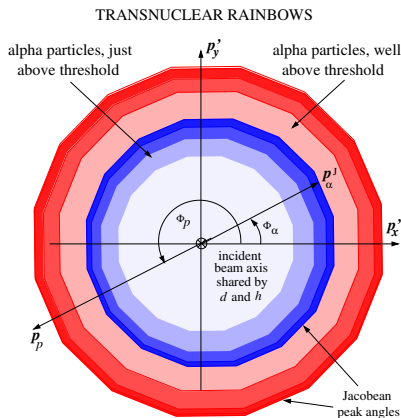
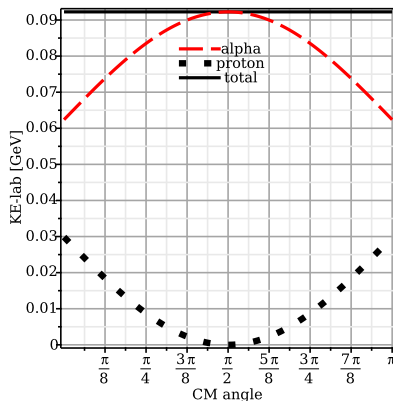


Figure 11: Transnuclear “rainbows” produced in the reaction $h + d \rightarrow \alpha + p$. Shading represents scattered differential cross section. Rainbow radii increase proportional to incident energy excess above threshold. Superscript “J” labels the rainbow divergence edge caused by the vanishing Jacobean at the maximum laboratory scattering angle.

24 Final state kinetic energies



- ▶ Relation between c.m angles and lab kinetic energies.
- ▶ that the process is exothermic is provided by the fact that the 92.2 GeV sum of kinetic energies the $49.0+24.9=73.9$ GeV sum of incident energies by 18.3 GeV.
- ▶ which is the exothermic energy

25 Phase space weighted kinetic energies

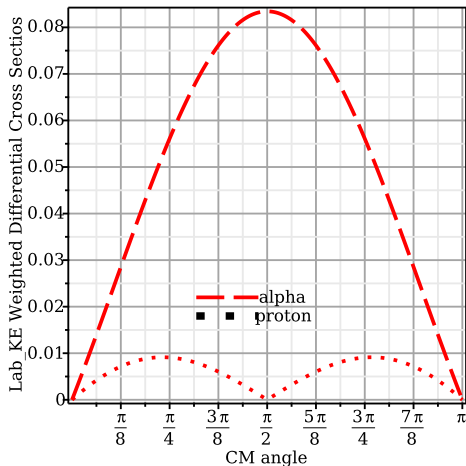


Figure 12: Weighted by the c.m. phase space density factor $\sin \theta_{c.m.}$, the radiated laboratory kinetic energy distributions of the secondary beams are plotted against c.m. angle.

26 Final state power distribution

- ▶ The proposed apparatus will control the incident polarizations and measure both scattered polarizations,
- ▶ For rate estimates it is sufficient to treat all particles as unpolarized, assuming incident spins are unpolarized and final state spins are not measured.
- ▶ The only need for quantum mechanical wave function Ψ is to provide a probabilistic conversion from wave amplitude, via wave intensity, to (point) particle probability distributions.
- ▶ The Fermi statistical model assumes only isotropic angular distribution, which are (almost) guaranteed by symmetry and conservation laws.
- ▶ Such cross section distributions are illustrated by color intensities in the rainbow figure.

27 Final state power distribution-continued

- ▶ Since the overall c.m is moving “forward” in the laboratory, these momenta will be forward-transformed, even to the extreme that the straight-backward heavy particle c.m. momentum points straight-forward in the laboratory.
- ▶ The transverse components of every particle will be fairly small, meaning that all particles are contained within fairly acute “rainbow” cones, such as illustrated in the figure.
- ▶ The rainbow rims, determined by Jacobean peaks, correspond to maximum transverse momentum in the c.m. system
- ▶ There is only one possible way in which the Fermi statistical model may not be quite correct.
- ▶ The maximum transverse momentum may not occur exactly at $\pi/2$ in the c.m. system

28 Estimated rate of power generation

- Possible parameters include

$$\begin{aligned}f_{\text{sr}} &= \text{storage ring revolution frequency} &&= 10^6 \text{ Hz}, \\N_d, N_h &= \text{numbers of stored particles} &&= 10^{10}, \\A_b &= \text{beam area} = 0.1 \text{ cm} \times 0.1 \text{ cm} &&= 10^{-2} \text{ cm}^2, \\\sigma &= \text{nuclear cross section} &&= 10^{-24} \text{ cm}^2,\end{aligned}$$

- The (deuterium) "target bunch nuclear opacity"

$$O_N = N_d \sigma / A_b = 10^{10} \times 10^{-24} / 10^{-2} = 10^{-12}, \quad (4)$$

gives the fraction of bunch passages which result in a nuclear transmutation event

- The rate of particle passages is

$$r_{\text{pass}} = \frac{f_{\text{sr}}}{7} N_h = \frac{10^6}{7} \times 10^{10} = 0.142 \times 10^{16} / \text{s}. \quad (5)$$

29 Estimated power production

- ▶ The nuclear transmutation event rate is

$$r_{\text{event}} = O_{\text{N}} \times r_{\text{pass}} = 10^{-12} \times 0.142 \times 10^{16} = 1.42 \times 10^3 / \text{s}. \quad (6)$$

- ▶ The conversion factor from MeV to Joule is $1.602 \times 10^{-13} \text{ J/MeV}$ and the maximum possible energy extraction is $Q_{D-\text{He3}} = 18.3 \text{ MeV/event}$.
- ▶ The power averaged over one second

$$P_{\text{average}} = 1.42 \times 10^3 \times 16.35 \times 1.602 \times 10^{-13} \text{ W}. \quad (7)$$

- ▶ From a nuclear power perspective this is utterly negligible, down by many orders of magnitude compared to the KW energy consumption rate of a typical individual.

30 Rate of isotope conversion events

- ▶ Negligible as power generation, the beam still circulates,
- ▶ and there is no power nor energy expended (at least in principle).
- ▶ One can even imagine top-off injection, allowing continuous colliding beam operation.
- ▶ The (previously calculated) event rate is

$$r_{\text{event}} = O_N \times r_{\text{pass}} = 10^{-12} \times 0.142 \times 10^{16} = 1.42 \times 10^3 / \text{s}, \quad (8)$$

- ▶ For fundamental physics this event rate of isotope conversions is the appropriate measure of productivity in studying spin dependence and measuring small branching fractions.
- ▶ This is a huge event rate, especially considering that the initial spin states can be pure, and the output polarizations can be measured, event by event.

31 The pure physics goal

- ▶ The real goal is to provide experimental data sufficient to refine our understanding of the nuclear force and nuclear physics.
- ▶ Pure incident spin states, high analyzing power final state polarization measurement, and high data rates should initiate a qualitatively and quantitatively new level of experimental observation of nuclear reactions.
- ▶ Precision measurement of inverse channels, such as $h + d \rightarrow \alpha + p$ and $\alpha + p \rightarrow h + d$ will test time reversal invariance.

32 Bunch passage remote from RF

BUNCHING of 2 BEAMS of DIFFERENT VELOCITY in SINGLE RF CAVITY

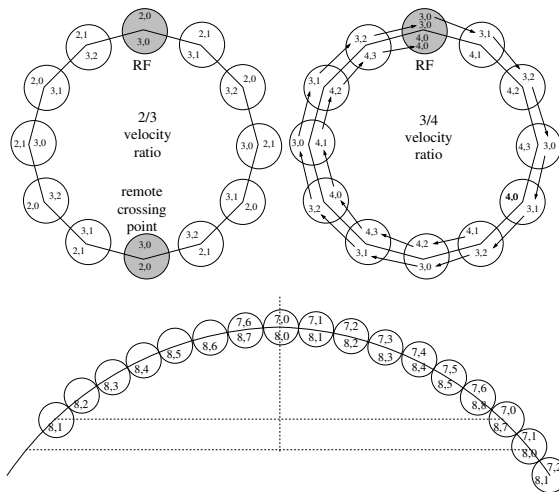


Figure 13: Stable RF buckets for beams of different velocity. Increasing the RF frequency introduces further potential remote IP locations.

33 Bunch passage remote from RF (continued)

- ▶ After 56 turns, both beams pass the RF system “in phase” and can therefore be bunched.
- ▶ By increasing the base frequency by a factor of 56, the same condition will be achieved after one turn.
- ▶ But the IP and RF positions are superimposed, which is unsatisfactory.
- ▶ By doubling the rf frequency, a remote location will open which can have IP optics optimized for luminosity, though still with some collisions occurring in the single RF.
- ▶ One could, however, go from one to two, symmetrically-located, phase-shifted RF cavities, effectively shifting the effective RF phase.
- ▶ Would this not allow RF phases to be shifted for their phasor sum to enable moving the IP's away from the physical RF's? It must be checked!

34 References

Thanks for your attention



R. Talman, *Superimposed Electric/Magnetic Dipole Moment Comparator Lattice Design*, ICFA Beam Dynamics Newsletter #82, Yunhai Cai, editor, Journal of Instrumentation, JINST_118P_0721, 2021



R. Talman, *Difference of measured proton and He3 EDMs: a reduced systematics test of T-reversal invariance*, Journal of Instrumentation, JINST_060P_0522, 2022



R. Talman, *Proposed experimental study of wave-particle duality in p,p scattering*, <https://arxiv.org/abs/2302.03557>, and Journal of Instrumentation, <https://pos.sissa.it/433/039/pdf>, 2023










CPEDM Group, *Storage ring to search for electric dipole moments of charged particles Feasibility study*, CERN Yellow Reports: Monographs, CERN-2021-003, 2021










E. Gibney, *Nuclear-fusion reactor smashes energy record*, Nature. doi:10.1038/d41586-022-00391-1, 2022



Wikipedia article, *Lawson criterion*

-  J.D. Lawson, *Some Criteria for a Power Producing Thermonuclear Reactor*, Proc. Phys. Soc., **B**, 70, (1), doi:10.1088/0370-1301/70/1/303, 1955
-  S.T. Butler, *Angular distribution from (d,p) and (d,n) nuclear reactions*, Proc. Roy. Soc. (London) **A208**, 559, 1951
-  V. B. Reva, *COSY experience of electron cooling*, 12th Workshop on Beam Cooling and Related Topics, COOL2019, Novosibirsk, Russia, JACoW Publishing, doi:10.18429/JACoW-COOL2019-MOX01, 2019
-  J. R. Oppenheimer and M. Phillips, Phys. Rev., **48**, 500, 1935
-  J.M. Blatt and V.F Weisskopf, *Theoretical Nuclear Physics*, p. 504, John Wiley and Sons, New York, 1952
-  S.T. Butler, *Direct nuclear reactions*, Phys. Rev., **106**, 1, 1957
-  E. Fermi, *High Energy Nuclear Events*, Progr. Theor. Physics **5**, 570, 1950

-  R. Hagedorn, *Relativistic Kinematics*, W. A. Benjamin, Inc., 1960
-  <https://home.cern/science/engineering/powering-cern>
-  C. Wilkin, *The legacy of the experimental hadron physics program at COSY*, Eur. Phys. J. A 53 (2017) 114, 2017
-  D. Eversmann et al., *New method for a continuous determination of the spin tune in storage rings and implications for precision experiments*, Phys. Rev. Lett. **115** 094801, 2015
-  N. Hempelmann et al., *Phase-locking the spin precession in a storage ring*, P.R.L. 119, 119401, 2017
-  F. Rathmann, N. Nikoliev, and J. Slim, *Spin dynamics investigations for the electric dipole moment experiment*, Phys. Rev. Accel. Beams 23, 024601, 2020
-  J. Slim et al., *First detection of collective oscillations of a stored deuteron beam with an amplitude close to the quantum limit*, Phys. Rev. Accel. Beams, 24, 124601, 2021



F. Rathmann, *First direct hadron EDM measurement with deuterons using COSY*, Willy Haeberli Memorial Symposium, <https://www.physics.wisc.edu/haeberli-symposium>, 2022



R. Talman, *Improving the hadron EDM upper limit using doubly-magic proton and helion beams*, arXiv:2205.10526v1 [physics.acc-ph] 21 May, 2022



R. Talman and N. N. Nikolaev, *Colliding beam elastic p, p and p, d scattering to test T - and P -violation*, Snowmass 2021, Community Town Hall/86, 5 October, 2020



P. Lenisa et al., *Low-energy spin-physics experiments with polarized beams and targets at the COSY storage ring*, EPJ Techniques and Instrumentation, <https://doi.org/10.1140/epjti/s40485-019-0051-y>, 2019